

# The transition state shape-selective aromatic alkylation over MnAPO-11 molecular sieve catalysts

Yong Hwa Yeom, Sang Chul Shim\*

Department of Chemistry, Center for Molecular Design and Synthesis and School of Molecular Science-BK21, Korea Advanced Institute of Science and Technology, Yusung-Gu, Taejon 305-701, South Korea

Received 2 April 2001; accepted 9 October 2001

## Abstract

MnAPO-11 molecular sieves with medium size elliptical pore are synthesized and characterized. Transition state shape-selective catalysis of these molecular sieves are studied. Methylation of alkylaromatic compounds were efficiently catalyzed by these molecular sieves while aromatic ethylation was almost negligible. The size of the alkylating agents was the key factor for the transition state dimension in the aromatic alkylation, not the size of aromatic compounds. The mole fraction of *o*-isomer for methylation of alkylaromatic compounds was dependent on the size of the alkyl groups. © 2002 Elsevier Science B.V. All rights reserved.

**Keywords:** MnAPO-11 molecular sieves; XRD and SEM; Diethylamine; Aromatic alkylation; Transition state

## 1. Introduction

Microporous crystalline aluminophosphate molecular sieves (AlPO-*n*, where *n* represents the type of structure) [1,2] can easily be modified by incorporating heteroatoms such as Si and transition metals at P (SAPO-*n*) and Al (MeAPO-*n*) [3,4]. The SAPO-*n* and MeAPO-*n* (Me: bivalent metal cations such as Mg<sup>2+</sup>, Mn<sup>2+</sup>, Co<sup>2+</sup>, Zn<sup>2+</sup>) are weakly acidic and have potential catalytic applications in petroleum refining and petrochemical processes [5].

AlPO-11, SAPO-11 and MeAPO-11 molecular sieves were synthesized utilizing dialkylamine templating agents such as di-*n*-propylamine and di-*i*-propylamine. These molecular sieves have one-dimensional

10-membered ring channels with an elliptical pore opening of 0.63 nm × 0.39 nm [6] while AlPO-5, SAPO-5 and MeAPO-5 molecular sieves have one-dimensional 12-membered ring channels with a circular pore opening of 0.73 nm × 0.73 nm [7].

Heteroatom incorporated SAPO-11 and MeAPO-11 molecular sieves showed shape-selective catalytic properties for the skeletal isomerization of butene-1 [8] and hydroisomerization of *n*-paraffins [9]. Butene-1 could be transformed into *i*-butene in the pore of SAPO-11 or MeAPO-11, but dimerization of butene isomers is suppressed. The primary products of hydroisomerization of *n*-paraffins over Pt/SAPO-11 are mono-methyl branched paraffins, while preferential hydrocracked and multibranched isomer products have been found for large-pore Pt/SAPO-5 catalyst.

In the present work, we report a synthesis, characterization and transition state shape-selective catalysis of MnAPO-11 molecular sieves.

\* Corresponding author. Tel.: +82-42-869-2815;

fax: +82-42-869-2810.

E-mail address: scshim@mail.kaist.ac.kr (S.C. Shim).

## 2. Experimental

### 2.1. Synthesis and characterization of AlPO-based molecular sieves

AlPO-based molecular sieves were synthesized by the hydrothermal method. Pseudoboehmite (Conoco; 71.7% Al<sub>2</sub>O<sub>3</sub>) or aluminum tri-*i*-propoxide (Aldrich; >98%), *o*-phosphoric acid (Kanto; 85%) and MnCl<sub>2</sub>·4H<sub>2</sub>O (Aldrich; >98%) were used as Al, P and Mn source, respectively. Diethylamine (Aldrich; >99.5%), di-*n*-propylamine (Aldrich; >99%), and tri-*n*-propylamine (Aldrich; >99%) were used as templating agents.

A 10-membered ring pore AlPO-11 was synthesized according to the literature method from di-*n*-propylamine (DPA), pseudoboehmite and *o*-phosphoric acid [2]. Pseudoboehmite was added to a mixture of phosphoric acid and water with vigorous stirring at room temperature for 5 h followed by addition of DPA with stirring and the resulting mixture was stirred for 4 h until it became a homogeneous gel. The molar composition of the gel was determined to be 1.3DPA:1.0Al<sub>2</sub>O<sub>3</sub>:1.0P<sub>2</sub>O<sub>5</sub>:40H<sub>2</sub>O.

This homogeneous gel mixture was transferred into Teflon lined stainless steel autoclave, heated in oven to 200 °C, and then left for 48 h. The products were filtered, washed and dried at 120 °C.

Eight kinds of MnAPO-11 were synthesized from different gel molar compositions and denoted MnAPO-11 (*x*DEA) and MnAPO-11 (*x*DPA). DEA represents diethylamine and the molar compositions of the MnAPO-11 gels are as follows:

MnAPO-11 (*x*DEA),  $x = 1.3, 1.6, 1.9, 2.2,$   $x\text{DEA} : 0.833\text{MnCl}_2 : 2.0\text{Al}(\text{O}-i\text{Pr})_3 : 1.0\text{P}_2\text{O}_5 : 40\text{H}_2\text{O}$

MnAPO-11 (*x*DPA),  $x = 1.3, 1.6, 1.9, 2.2,$   $x\text{DPA} : 0.833\text{MnCl}_2 : 2.0\text{Al}(\text{O}-i\text{Pr})_3 : 1.0\text{P}_2\text{O}_5 : 40\text{H}_2\text{O}$

These homogeneous gel mixtures were heated at 200 °C for 72 h.

A 12-membered ring pore MnAPO-5 was synthesized according to the literature by using tri-*n*-propylamine (TPA), pseudoboehmite and *o*-phosphoric acid [4]. The molar gel composition and reaction conditions are as follows: 1.3TPA:0.833MnCl<sub>2</sub>:1.0Al<sub>2</sub>O<sub>3</sub>:1.0P<sub>2</sub>O<sub>5</sub>:40H<sub>2</sub>O, 160 °C and 48 h.

Synthesized molecular sieve products were characterized by X-ray diffraction (XRD, Rigaku 3D/Max-C) using Cu K $\alpha$  radiation, scanning electron microscopy

(SEM, Philips XL30SFEG) and thermogravimetric analysis (TGA, Perkin-Elmer TGA-7). TGA experiments were performed with 10 °C/min increasing rate of temperature in the N<sub>2</sub> flow. Al, P and Mn contents were determined using inductively-coupled plasma mass spectrometer (ICP/MS, Hewlett-Packard HP4500).

### 2.2. Catalytic reactions

Catalytic tests in a continuous flow were performed with a fixed bed reactor. The catalysts were loaded in the half-inch stainless steel tube surrounded by furnace and purged with 20 ml/min N<sub>2</sub> gas at the reaction temperature for 1 h. The flow of the gas and liquid reactants was controlled by thermal mass flow controller and syringe pump, respectively.

Synthesized molecular sieves were calcined at 550 °C for 12 h to remove organic templating agents and were used as catalysts. Aromatic alkylation reactions were carried out under the following conditions:

- amount of catalyst: 400 mg;
- aromatic reagents: toluene, ethylbenzene, *n*-propylbenzene, cumene;
- alkylating agents: MeOH or EtOH;
- aromatics/alkylating agent/N<sub>2</sub>: 1/1/5 (molar ratio);
- reaction temperature, pressure: 400 °C, 1 bar;
- feeding rate: 2/h for toluene as weight hourly space velocity (WHSV).

The products were trapped with ice bath and analyzed by GC utilizing a HP-FFAP capillary column.

## 3. Results and discussion

### 3.1. Characterization

#### 3.1.1. XRD and SEM studies

The position of the peaks in all eight MnAPO-11 was identical to the literature values [10] and the XRD patterns of representative four MnAPO-11 are shown

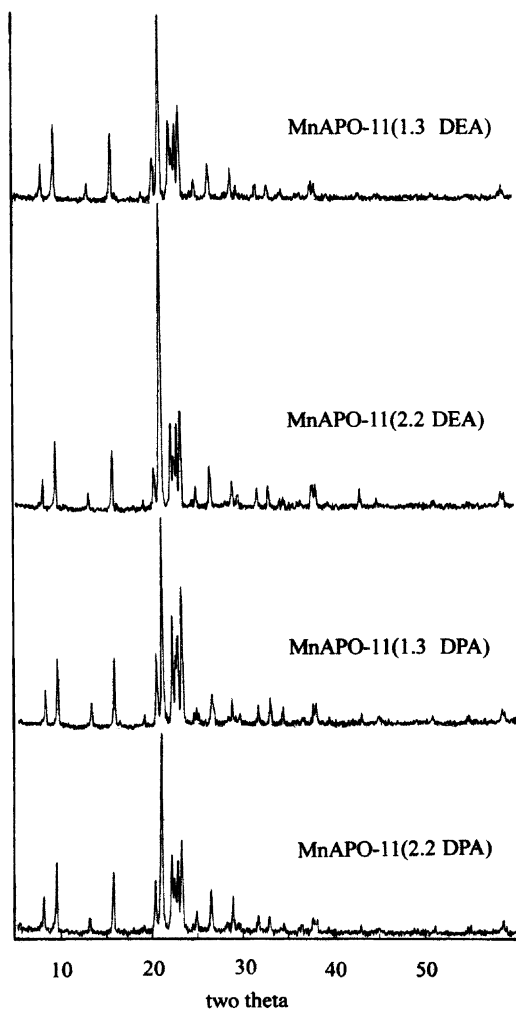


Fig. 1. XRD patterns of MnAPO-11.

in Fig. 1. The relative peak intensity is very similar to each other for MnAPO-11 (1.3DEA), MnAPO-11 (1.3DPA) and MnAPO-11 (2.2DPA). However, the relative peak intensity for  $21.0^\circ$  of  $2\theta$  value in MnAPO-11 (2.2DEA) is very strong suggesting very different crystal shape. The X-ray is randomly diffracted by crystal particles and the intensity of specific peak is proportional to the exposure probability of its corresponding crystal plane. The strong peak for  $21.0^\circ$  of  $2\theta$  value in MnAPO-11 (2.2DEA), therefore, is the result of strong and selective XRD by a particular plane of the crystal suggesting a thin plate crystal structure for MnAPO-11 (2.2DEA).

The XRD pattern of MnAPO-5 was in good agreement with the reported results [11].

SEM images of synthesized MnAPO-11 samples show different morphology from each other as shown in Fig. 2. The shape of the crystal is of polycrystalline thin plate aggregates and the thickness of the plate is about  $0.5\ \mu\text{m}$  for MnAPO-11 (1.3DEA). The crystal is of separated thin plate with sizes from 15 to  $20\ \mu\text{m}$  for MnAPO-11 (2.2DEA) and the thickness of the plate is about  $1\ \mu\text{m}$ . The shape of the crystal is of polycrystalline aggregates for MnAPO-11 (1.3DPA) and MnAPO-11 (2.2DPA) with the primary particle size of MnAPO-11 (2.2DPA) being smaller than that of MnAPO-11 (1.3DPA). The shape of the particle is closely correlated with the XRD peak intensity confirming the thin plate crystal structure for MnAPO-11 (2.2DEA). The peak for  $21.0^\circ$  of  $2\theta$  value is matched to the (002) plane which is perpendicular to the direction of one-dimensional channel [10].

### 3.1.2. Chemical composition

The chemical composition of each molecular sieve is shown in Table 1. The molar ratio of P is slightly larger than that of Al plus Mn for MnAPO-11. For MnAPO-5, the molar ratio of P is nearly the same as that of Al plus Mn. The result indicates that bivalent Mn is incorporated into the trivalent Al site.

### 3.1.3. TGA analysis

The AlPO-11 shows one-step weight loss in the temperature region around  $200^\circ\text{C}$  while two-step weight losses in the temperature regions around 200 and  $350^\circ\text{C}$  are observed in MnAPO-11 (1.3DEA) as shown in Fig. 3. The weight loss is due to the decomposition of organic templating agents filling the pore. The charge of AlPO-11 framework is neutral and the organic amines are filled physically in the pore which are removed from the pore at around  $200^\circ\text{C}$ . It has

Table 1  
Chemical analysis data (molar ratio)

Catalyst	Composition of $\text{Mn}_x\text{Al}_y\text{P}_z\text{O}_4$			
	x	y	z	x + y/z
MnAPO-11 (1.3DPA)	0.057	0.91	1.03	0.94
MnAPO-11 (1.3DEA)	0.056	0.92	1.02	0.96
MnAPO-5	0.058	0.95	1	1.01

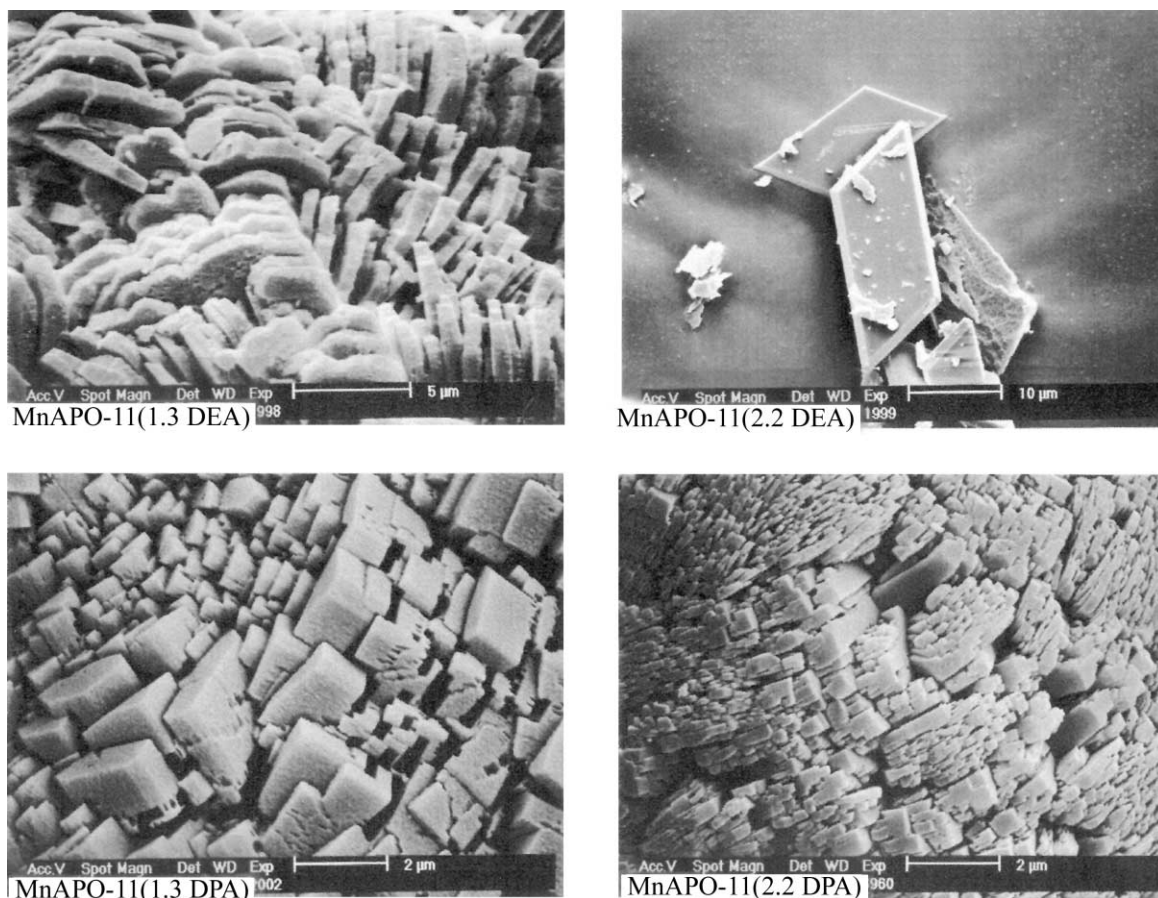


Fig. 2. SEM images of MnAPO-11.

been reported that bivalent metal-substituted crystalline aluminophosphates have negative framework charge and Lewis acidity (12). The organic amines interact strongly with the Lewis acidic framework and are removed from the pore at higher temperature (350 °C).

### 3.2. Transition state shape-selective catalytic reactions

#### 3.2.1. Methylation of toluene

Table 2 shows the results of methylation of toluene over AlPO-11, MnAPO-11 (1.3DPA) and MnAPO-5 catalysts. AlPO-11 has no acidic site and shows negligible catalytic activity. On the other hand, MnAPO-11 and MnAPO-5 show mild catalytic activity because

Table 2  
The yield of methylation of toluene (reaction time: 2 h)

Product	Catalyst		
	AlPO-11	MnAPO-11 (1.3DPA)	MnAPO-5
Benzene	–	–	0.5
Ethylbenzene	–	>0.1	>0.1
<i>p</i> -Xylene	0.1	5.2 (40) <sup>a</sup>	2.1 (28)
<i>m</i> -Xylene	>0.1	5.6 (43)	3.2 (42)
<i>o</i> -Xylene	>0.1	2.3 (17)	2.3 (30)
Trimethylbenzene	–	2.4	1.7
Others	–	0.2	0.7
Conversion (%)	0.1	15.8	10.6

<sup>a</sup> Fraction of isomers.

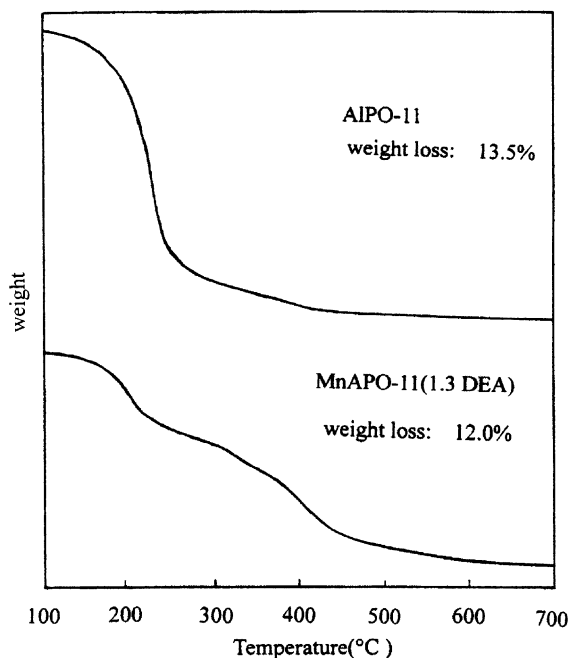


Fig. 3. TGA of AIPO-11 and MnAPO-11.

they have Lewis acid sites generated from the Mn replacement for Al site [12]. The mechanism of aromatic alkylations over molecular sieve catalysts was reviewed by Venuto [13]. The alkylation proceeds through electrophilic addition of a carbenium ion generated from alkylating agent. It is well known that *p*-*o*-substitution is strongly favored over *m*-substitution in the electrophilic alkylation of alkylaromatics because of electron-releasing effect of alkyl group [14]. The *m*-isomer is formed from *p*- and *o*-isomers through isomerization, not by direct alkylation. The sum of the mole fractions of *p*- and *o*-isomers for MnAPO-11 (1.3DPA) is nearly equal to that of MnAPO-5 and the mole fraction of *m*-isomer is almost equal for both catalysts indicating that the isomerization reactivity of two catalysts is very similar to each other. The *p*-*o*-isomer ratio of MnAPO-5 is 28/30 while that of MnAPO-11 (1.3DPA) is 40/17. The results can be correlated to the diffusion characteristics of *p*- and *o*-isomer in the micropore. The pore size of MnAPO-5 is 0.73 nm × 0.73 nm which is larger than the molecular dimension of xylene isomers and the diffusivity difference of xylene isomers is small. But, the pore size of MnAPO-11 is 0.63 nm × 0.39 nm

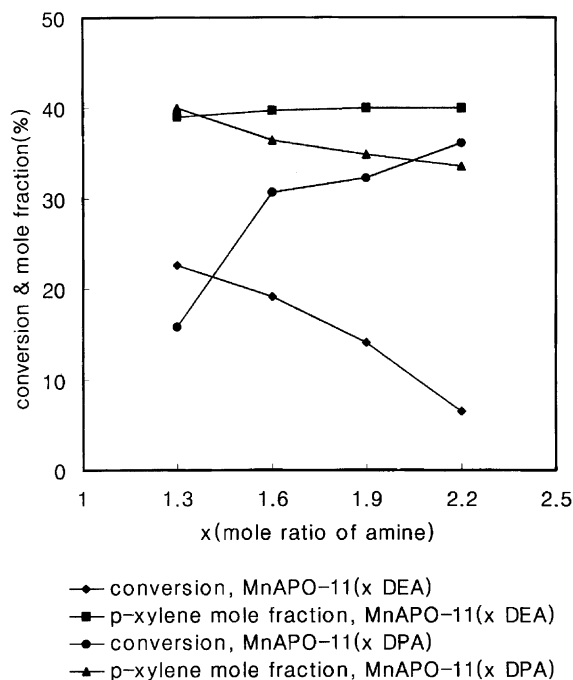


Fig. 4. Methylation of toluene over MnAPO-11.

which is close to the molecular dimension of xylene isomers and the diffusivity of *p*- and *o*-xylene is different. The diffusion coefficient of *p*-xylene in the pore of AIPO-11 at 90 °C is  $4 \times 10^{-12}$  cm<sup>2</sup>/s and that of *o*-xylene is  $2 \times 10^{-12}$  cm<sup>2</sup>/s [15]. The *p*-xylene mole fraction is, therefore, high for MnAPO-11. Benzene is formed over MnAPO-5 but not over MnAPO-11 (1.3DPA) due to the transition state shape-selectivity. Benzene could be formed by transalkylation of toluene. The pore size of MnAPO-11 (1.3DPA) is not large enough for the accommodation of transition state but that of MnAPO-5 is.

The extent of conversion and the mole fraction of *p*-xylene for the methylation of toluene over MnAPO-11 (*x*DEA) and MnAPO-11 (*x*DPA) catalysts are plotted in Fig. 4. The catalytic activity of MnAPO-11 (*x*DEA) was decreased as the mole fraction *x* of amines are gradually increased while that of MnAPO-11 (*x*DPA) catalysts was increased. The differences can be explained by the size and shape of MnAPO-11 crystallites. As shown in Fig. 2, the crystal size and plate thickness of MnAPO-11 (*x*DEA) with large *x*-values is larger than those of MnAPO-11

( $x$ DEA) with small  $x$ -values. For large crystallite, the rate of coming in and out of reactant and product molecules to catalytic site in the pore is slow and reaction is suppressed. But, the order for crystal size of MnAPO-11 ( $x$ DPA) is opposite to that of MnAPO-11 ( $x$ DEA) and the reactivity of MnAPO-11 ( $x$ DPA) with large  $x$ -values is higher than that of MnAPO-11 ( $x$ DPA) with small  $x$ -values. The mole fraction of  $p$ -xylene generated over MnAPO-11 ( $x$ DEA) catalysts were nearly equal regardless of  $x$ -values, but small for MnAPO-11 ( $x$ DPA) with large  $x$ -values because additional isomerization to  $m$ -xylene takes place more actively for small crystallite MnAPO-11 catalysts. The basic catalytic properties of MnAPO-11 catalysts are nearly equal regardless of DEA and DPA as templating agents. The reactivity difference of MnAPO-11 ( $x$ DEA) and MnAPO-11 ( $x$ DPA) catalysts can be attributed to the physical properties such as crystal shape and size rather than the chemical properties.

### 3.2.2. Ethylation of toluene and methylation of ethylbenzene

Ethylation of toluene and methylation of ethylbenzene produce ethyltoluene isomers (Tables 3 and 4). The methylation of ethylbenzene is 2.2 times faster than the methylation of toluene (Table 2) over MnAPO-11 (1.3DPA) catalyst. The electron-releasing effect of ethyl group is higher than that of methyl group. The activation energy of transition state formation is expected to be lower for ethylbenzene than toluene leading to the higher reactivity for ethylbenzene. But, the ethylation of toluene is nearly negligible over MnAPO-11 (1.3DPA) catalyst. This result is

Table 3  
The yield of ethylation of toluene (reaction time: 2 h)

Product	Catalyst		
	AlPO-11	MnAPO-11 (1.3DPA)	MnAPO-5
Benzene	–	–	1.2
Ethylbenzene	–	0.05	2.6
Xylenes	0.05	–	4.1
<i>p</i> -Ethyltoluene	–	0.15	6.0 (36.6) <sup>a</sup>
<i>m</i> -Ethyltoluene	–	0.1	8.0 (48.8)
<i>o</i> -Ethyltoluene	–	–	2.4 (14.6)
Others	–	–	2
Conversion (%)	0.05	0.3	26.3

<sup>a</sup> Fraction of isomers.

Table 4

The yield of methylation of ethylbenzene (reaction time: 2 h)

Product	Catalyst	
	MnAPO-11 (1.3DPA)	MnAPO-5
Benzene	>0.1	1.4
Toluene	0.1	1.4
Xylenes	0.2	1.2
<i>p</i> -Ethyltoluene	11.4 (43.2) <sup>a</sup>	2.0 (33.3)
<i>m</i> -Ethyltoluene	12.5 (47.3)	2.8 (46.7)
<i>o</i> -Ethyltoluene	2.5 (9.5)	1.2 (20.0)
<i>p</i> -Diethylbenzene	–	2
<i>m</i> -Diethylbenzene	–	1.1
<i>o</i> -Diethylbenzene	–	0.1
Dimethylethylbenzene	7.2	0.6
Others	0.6	0.7
Conversion (%)	34.6	14.5

<sup>a</sup> Fraction of isomers.

attributed to the transition state shape-selective catalysis of which a model is shown in Fig. 5. The empty  $\pi$ -orbital of carbenium ion formed from alkylating agent (alcohol) overlaps and interacts with  $\pi$ -electrons of aromatic ring and the aromatic compound is laid on top of the carbenium ion. The MnAPO-11 has elliptical 0.63 nm  $\times$  0.39 nm size pore which can accommodate the transition state for methylation of aromatic compounds but not for the ethylation because of the large steric hindrance. The size of aromatic reactants and products exerts negligible effect on the reactivity but the size of the alkylating agent is the critical factor in the aromatic alkylation over MnAPO-11 catalyst. The transition state shape-selective catalysis over MnAPO-11 (1.3DPA) is correlated with the absorbing characteristics. The 0.63 nm  $\times$  0.39 nm size pore can absorb xylene isomers and trimethylbenzene isomers which are planar but cannot absorb cyclohexane which has non-planar chair structure with axial hydrogens [15]. The short 0.39 nm pore dimension cannot accommodate the transition state for aromatic ethylation as well as non-planar cyclohexane molecule. The mole fraction of *o*-ethyltoluene over MnAPO-11 (1.3DPA) catalyst (Table 4) is 9.5% which is much smaller than that of *o*-xylene and half of thermodynamic equilibrium mole fraction value. The *p*-/*o*-isomer ratio of MnAPO-11 (1.3DPA) catalyst is 2.4 for toluene methylation and 4.5 for ethylbenzene methylation. This result is correlated with transition state of the reaction. Ethyl group

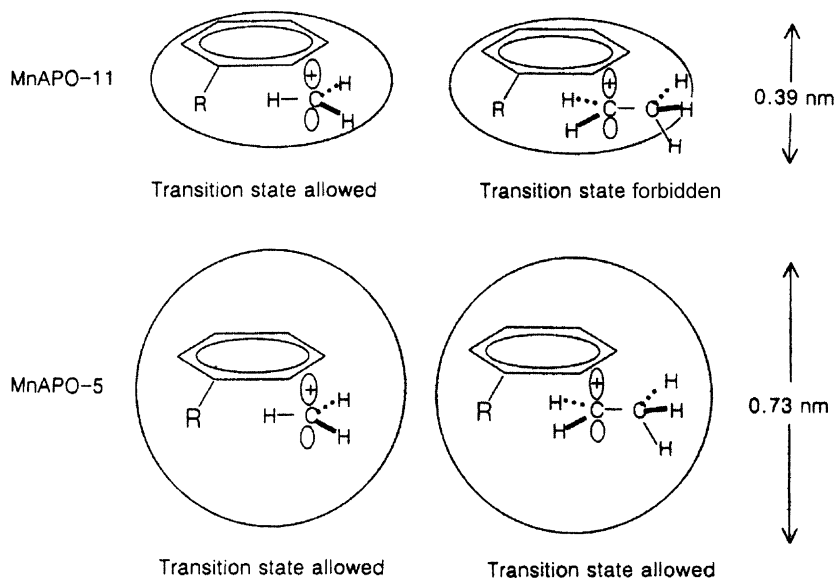


Fig. 5. Transition states for aromatic alkylation.

is larger than methyl group and prefer *p*-substitution than *o*-substitution. On the other hand, MnAPO-5 catalyst shows considerable reactivity for both the ethylation of toluene and the methylation of ethylbenzene. As shown in Fig. 5, the pore size of MnAPO-5 is  $0.73 \text{ nm} \times 0.73 \text{ nm}$  which can accommodate the transition states for both methylation and ethylation of aromatic compounds. The ethylation of toluene is 2.5 times faster than the methylation of toluene (Table 2) probably due to the difference in the rate of the corresponding ethyl and methyl carbenium ion formation. The ethyl carbenium ion is more stable and formed faster than methyl carbenium ion. The methylation of ethylbenzene is 1.4 times faster than the methylation of toluene (Table 2) probably due to the difference of electron releasing effect of methyl and ethyl group.

### 3.2.3. Methylation of *n*-propylbenzene and cumene

Table 5 shows the results for methylation of *n*-propylbenzene and cumene over MnAPO-11 (1.3DPA) catalyst. The methylation of *n*-propylbenzene is slightly faster than methylation of ethylbenzene probably due to the stronger electron releasing property of *n*-propyl group than that of ethyl group. The mole fraction of *o*-isomer in the methylation of *n*-propylbenzene is 10.0% and very similar to the methylation

of ethylbenzene. The *n*-propyl and ethyl group are primary alkyl groups and the size effect of alkyl groups for transition state of *o*-substitution is similar to each other. The methylation of cumene is much slower than methylation of *n*-propylbenzene. The reactivity difference can be explained by the cracking reactions. The formation of benzene is nearly negligible in methylation of *n*-propylbenzene while considerable

Table 5

The yield of methylation over MnAPO-11 (1.3DPA) (reaction time: 2 h)

Product	Reactant	
	<i>n</i> -Propylbenzene	Cumene
Benzene	>0.1	1.4
Toluene	0.3	0.8
Xylenes	0.2	0.4
<i>p</i> - <i>n</i> -Propyltoluene	13.9 (47.9) <sup>a</sup>	–
<i>m</i> - <i>n</i> -Propyltoluene	12.2 (42.1)	–
<i>o</i> - <i>n</i> -Propyltoluene	2.9 (10.0)	–
<i>p</i> - <i>i</i> -Propyltoluene	–	5.6 (47.0)
<i>m</i> - <i>i</i> -Propyltoluene	–	6.1 (51.3)
<i>o</i> - <i>i</i> -Propyltoluene	–	0.2 (1.7)
Others	10.8	1.3
Conversion (%)	40.4	15.8

<sup>a</sup> Fraction of isomers.

in methylation of cumene. The formation of carbenium cation is dominant in the methylation of *n*-propylbenzene. On the other hand, cumene and methanol interact competitively with catalytic sites and the formation of methylated product is suppressed and the formation of cracked product (benzene) is promoted for methylation of cumene. The mole fraction of *o*-isomer for methylation of cumene is only 1.7% and attributed to the very large steric hindrance effect of secondary *i*-propyl group for the transition state of *o*-substitution. The size of alkyl group attached to aromatic ring is the key factor determining the *o*-isomer mole fraction and can be explained by the transition state shape-selective catalysis.

#### 4. Conclusions

MnAPO-11 molecular sieves with medium size elliptical pore were successfully synthesized by using diethylamine and di-*n*-propylamine in highly pure crystalline state. The shape of crystalline MnAPO-11 obtained from diethylamine is thin plate form in which the plane is perpendicular to channel direction and the thickness of the plate is the length of the channel formed.

The reactivity difference for the methylation of toluene over MnAPO-11 catalysts is related with the size of crystallite. Methylation of alkyl aromatic compounds was efficiently catalyzed by MnAPO-11 catalysts but aromatic ethylation was almost negligible. The difference of the reactivity is attributed to the dimension of the transition state for alkylations and the size of alcohol molecules is the key factor for the transition state dimension. The mole fraction of

*o*-isomer for methylation of alkylaromatic compounds was dependent on the size of the alkyl groups.

#### Acknowledgements

This investigation was supported by the Korea Electric Power Company endowment fund to the Korea Advanced Institute of Science and Technology.

#### References

- [1] S.T. Wilson, B.M. Lok, E.M. Flanigen, US Patent 4,310,440 (1982).
- [2] S.T. Wilson, B.M. Lok, C.A. Messina, T.R. Cannan, E.M. Flanigen, *J. Am. Chem. Soc.* 104 (1982) 1146.
- [3] B.M. Lok, C.A. Messina, R.L. Patton, R.T. Gajek, T.R. Cannan, E.M. Flanigen, US Patent 4,410,871 (1984).
- [4] S.T. Wilson, E.M. Flanigen, *Eur. Patent* 132,708 (1985).
- [5] J.A. Rabo, R.J. Pellet, P.K. Coughlin, E.S. Shamsoum, *Stud. Surf. Sci. Catal.* 46 (1989) 1.
- [6] J.M. Bennett, J.W. Richardson Jr., J.J. Pluth, J.V. Smith, *Zeolites* 7 (1987) 160.
- [7] J.M. Bennett, J.P. Cohen, E.M. Flanigen, J.J. Pluth, J.V. Smith, *ACS Symp. Ser.* 218 (1983) 109.
- [8] S. Yang, J. Lin, D. Guo, S. Liaw, *Appl. Catal. A: Gen.* 181 (1999) 113.
- [9] J.M. Campelo, F. Lafont, J.M. Marinas, *Appl. Catal. A: Gen.* 170 (1998) 139.
- [10] J.J. Pluth, J.V. Smith, J.W. Richardson Jr., *J. Phys. Chem.* 92 (1988) 2734.
- [11] S. Qui, W. Pang, H. Kessler, J.L. Guth, *Zeolites* 9 (1989) 440.
- [12] J. Janchen, M.J. Haanepen, M.P.J. Peeters, J.H.M.C. van Wolput, J.P. Wolthuisen, J.H.C. van Hooff, *Stud. Surf. Sci. Catal.* 84 (1994) 373.
- [13] P.B. Venuto, *Micropor. Mater.* 2 (1994) 297.
- [14] A. Corma, F. Llopi, F. Melo, P. Viruela, Zicovich-Wilson, *J. Am. Chem. Soc.* 116 (1994) 134.
- [15] H. Chon, *Catal. Sci. Tech.* 1 (1991) 91.